Experimental Verification of an Analytical Model of Filtering Impact on Coherent Digital Subcarriers Systems

Experimental Verification of an Analytical Model of Filtering Impact on Coherent Digital Subcarriers Systems

P. Torres-Ferrera[1,*], G. Parisi[1], J. Sime[1], C. Castro[1], R. Gaudino[2], G. Rizzelli[2], F. Pevere[3], M. S. Erkilinç[3], T. Duthel[1], C. Fludger[1] and A. Napoli[1]

[1] Infinera, Germany; [2] Politecnico di Torino, Italy; [3] Infinera, Sweden

[*]ptorresferre@infinera.com

Abstract: We present the experimental verification of a developed analytical model to estimate the filtering penalty in digital subcarrier coherent systems, reporting a high model accuracy with a maximum error in sensitivity penalty of 0.4 dB.

1. Introduction

The increasing demand for higher data rates in optical networks requires the adoption of more advanced technologies. Coherent detection, initially used in long-haul systems, is now entering the metro market and also being explored for shorter-reach networks like access segments. This shift is also driven by the potential for network restructuring, such as metro-access convergence and longer-reach Passive Optical Networks (PONs) [1].

Coherent systems offer advantages like increased receiver sensitivity and reach, but its adoption, in the aforementioned scenarios, introduces unique challenges. Metro links include in-line optical amplifiers, limiting their performance mainly due to Amplified Spontaneous Emission (ASE) noise and non-linear interference. Access networks, on the other hand, operate without in-line amplifiers, leading to low receiver power regimes and increased susceptibility to transceiver noise. In both cases, high-capacity transmission is affected by filtering originated from band-limited transceivers and ROADMs in metro segments and potential future metro-access.

Novel quality of transmission (QoT) estimation tools, tailored for the aforementioned scenarios, are then required for network design and dimensioning. Previous analytical models for filtered linear coherent systems have been presented for single-carrier dominated by ASE [2], single-carrier impacted by ASE and transceiver (TRX) noise [3], and for Digital Subcarrier Multiplexing (DSCM) transmission [4,5]. The latter has been verified against numerical simulations only. In this work, we perform the first experimental verification, to our knowledge, of an analytical model of linear DSCM-based coherent transmission affected by filtering, linear cross-talk (XT) and optical and electrical noise. We also extend the modelling from our previous work [5] by introducing new transceiver noise considerations arising from experimental observations.

2. Experimental setup

We show in Fig. 1(a) the experimental setup. We test a 400 Gbps transmission using a real-time DSCM-based coherent TRX [6], which operates with 16 Digital Subcarriers (DSCs) using DP-16-QAM format and Root Raised Cosine (RRC) pulse-shaped with a roll-off factor $\rho = 1/24$. The total symbol rate is 60 GBaud, the frequency spacing between DSCs is $\Delta f = 4$ GHz and the guard-band between DSCs is $\sim$100 MHz.

We introduce the optical filtering by loading Super-Gaussian filter (SGF) power profiles $T_{SGF}(f)$, each generated using Eq. 1 with a nominal -3 dB bandwidth equal to B and order z =3, into a programmable Wave Shaper.

$$T_{SGF}(f),\mathrm{dB} = 20\log_{10}(H_C(f)) = 20\log_{10}\left(\exp\left(-\ln(\sqrt{2})\cdot(2|f|/B)^{2z}\right)\right) \quad (1)$$

We tested SGFs with nominal values of B = 48 GHz, 54 GHz, 60 GHz and "∞" (i.e. no filtering). To illustrate the filtering effect in the DSCM signal, in Figs. 1(b) and (c) we show its optical spectrum without and with a B = 54 GHz optical filter, respectively. In Fig. 1(d), we show the loaded nominal filter profiles and the measured ones. We observe a difference between nominal and measured profiles which is due to the finite granularity of the Wave Shaper to generate the optical filter. Then, based on the measured profiles, in the analytical model we set the filters bandwidth equal to B_a = [45.6 GHz, 51.3 GHz, 57 GHz] with corresponding order of z_a = [2.5, 2.5, 2.6], instead of the nominal ones (i.e. B = [48 GHz, 54 GHz, 60 GHz] and z = [3, 3, 3], respectively).

The ASE noise is added after filtering, which is the worst-case situation in terms of performance penalty [2]. We set the Optical Signal-to-Noise-Ratio (OSNR) using a variable optical attenuator (VOA$_N$). We measure the OSNR with an optical spectrum analyzer, using as a reference bandwidth the DSCM symbol rate (R_S). Then, a second attenuator (VOA$_{RX}$) is used to set the signal received optical power (P_S^{RX}). After coherent reception and

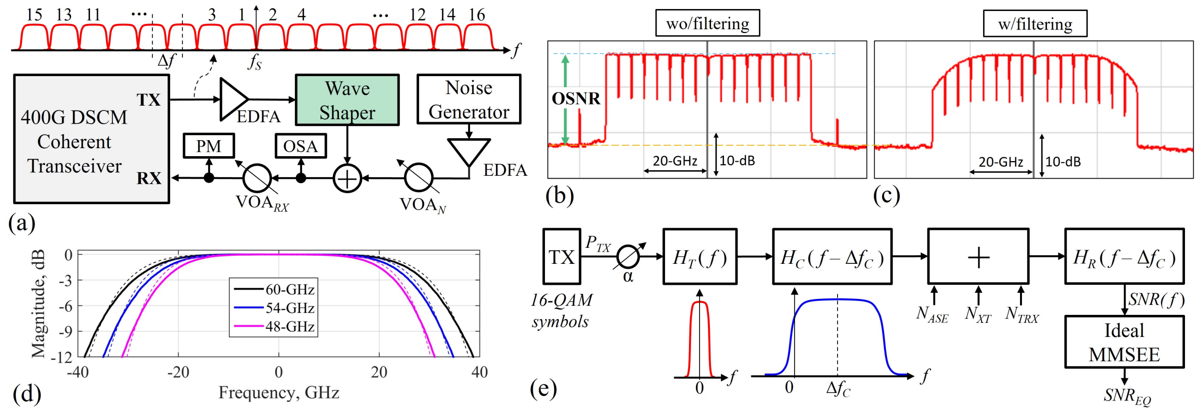

Fig. 1: (a) Experimental setup (PM: Power Meter). (b)-(c) Optical spectra (centered at f_S = 193.4 THz): (b) without filtering and (c) with filtering (B = 54 GHz). (d) Nominal (dashed) and measured (solid) filter profiles loaded to and generated by the Wave Shaper. (e) Block-diagram abstraction for analytical modelling on each subcarrier.

digital signal processing, the bit error ratio (BER) is calculated in real-time by the TRX. To properly compare the performance with and without filtering, in all conditions the reported OSNR is the average among DSCs when the filtering is absent, as shown in Fig. 1(b). The OSNR reduction of some DSCs after optical filtering results in a BER degradation of them, with a related sensitivity penalty, which is measured and estimated in next sub-sections.

3. Analytical modelling

We display in Fig. 1(e) the block-diagram we use in the analytical modelling. We extend the filtering model for DSCM signals presented in [5] to include a more complete transceiver noise model to match the experimental results. The rest of the model assumptions remains as in [5]. We recall the expression to compute the frequency resolved Signal-to-Noise-Ratio (SNR) of the i-th DSC ($SNR_i(f)$) at the receiver using Eq. 2.

$$SNR_i(f) = \frac{P_{S,i}(f)}{P_{N,i}(f)} = \frac{P_{S,i}^{RX} \cdot |H_T(f) \cdot H_C(f-\Delta f_{C,i}) \cdot H_R(f-\Delta f_{C,i})|^2}{N_{TRX,i}(f) + N_{ASE,i}(f) + N_{XT,i}(f)} \tag{2}$$

where $P_{S,i}(f)$ is the received signal power spectrum of the i-th DSC, $P_{S,i}^{RX} = \alpha P_{TX,i}$ is the coherent received power per DSC (without filtering), $P_{TX,i}$ is the transmitted power per DSC, α is an attenuation factor, $H_T(f)$ and $H_C(f)$ are respectively the signal pulse shaping profile and the frequency response of the SGF used to investigate the filtering penalty. As in [3], we introduce here the frequency response of the receiver, $H_R(f)$, approximated as a 68-GHz SGF of order 6, used to remove out of band noise and spectral replicas. $N_{ASE,i}(f) = P_{S,i}^{RX} \cdot H_R(f)/\mathrm{OSNR}$ is the power of the ASE noise in the link (filtered by the receiver), with the OSNR defined on a bandwidth equal to R_S. The linear XT affecting each DSC, $N_{XT,i}$, is evaluated using Eq. 3 of [5]. The frequency shift $\Delta f_{C,i}$ is equal to minus the central frequency of the i-th DSC in baseband, for instance, Δf_C =30, 2, -2 and -30 GHz for DSC #15, #1, #2 and #16, respectively (see the DSC indexing at the top of Fig. 1(a)).

The power of the TRX noises is approximated as $N_{TRX,i}(f) = N_0 \cdot R_S + \beta \cdot P_{S,i}(f)$ [7]. $N_0 \cdot R_S$ is the signal independent component of N_{TRX} (accounting mainly from thermal and shot noise with PSD equal to N_0). The addition of the signal dependent noise component $\beta \cdot P_{S,i}(f)$, as detailed in [7], is the main upgrade of our model with respect to [5]. The value of β is found by fitting, equal to 15.1×10^{-3}, a value close to that reported in [1] (i.e. $1/\beta = 18.2$ dB). At the receiver output, assuming that it performs linear analog-to-digital conversion and ideal minimum mean square error equalization (MMSEE), we compute the SNR of the i-th DSC at the equalizer output, $SNR_{EQ,i}$, following Eq. 3 [8].

$$SNR_{EQ,i} = \left(T \cdot \int_{-\frac{1}{2T}}^{\frac{1}{2T}} \left(1 + \overline{SNR_i}(f)\right)^{-1} df \right)^{-1} - 1 = \left(T \cdot \int_{-\frac{1}{2T}}^{\frac{1}{2T}} \left(1 + \sum_{\mu} SNR_i\left(f - \frac{\mu}{T}\right)\right)^{-1} df \right)^{-1} - 1 \tag{3}$$

where μ is the integer number of spectral foldings, and T is the DSC symbol period. From $SNR_{EQ,i}$ we can calculate the corresponding pre-FEC BER_i for a given modulation format via well-known theoretical expressions. For 16-QAM, the relation is $BER_i = (3/8) \cdot \mathrm{erfc}(\sqrt{SNR_{EQ,i}/10})$, which allows to reproduce the sensitivity curves per DSC as BER_i versus $P_{S,i}^{RX}$. We present the sensitivity penalty [3] per DSC (ΔP_i) as a QoT metric. This ΔP_i is the extra signal receiver power needed to achieve the same performance (i.e., the same BER target, equal to 1.78×10^{-2}) as the reference case in the absence of filtering and ASE noise.

4. Experimental results

In Fig. 2 we report the experimental measurements compared to the analytical estimations. The evaluated sensitivity penalty is plotted as a function of the OSNR for representative DSCs and the four nominal filter bandwidths. In all cases, the analytical results (in lines) match well the experimental ones (in markers), thus showing a high accuracy of the analytical model, with a negligible error in most of the cases and a maximum error of 0.4 dB, only for the case of the outer DSCs and $B = 60$ GHz.

From the sensitivity plots, we can observe a performance degradation of the outer DSCs with respect to the central ones (not affected by filtering). This sensitivity degradation is different depending on the filter bandwidth. All these effects are accurately captured by the proposed model.

Note that the penalty of the outer DSCs, spectrally symmetrical with respect to the signal center frequency, is not fully identical. Instead, there is a slight difference between them which is due to a small frequency offset in the experiments between the signal center frequency and the filters center frequency of 0.1 GHz, properly set in the analytical model as well.

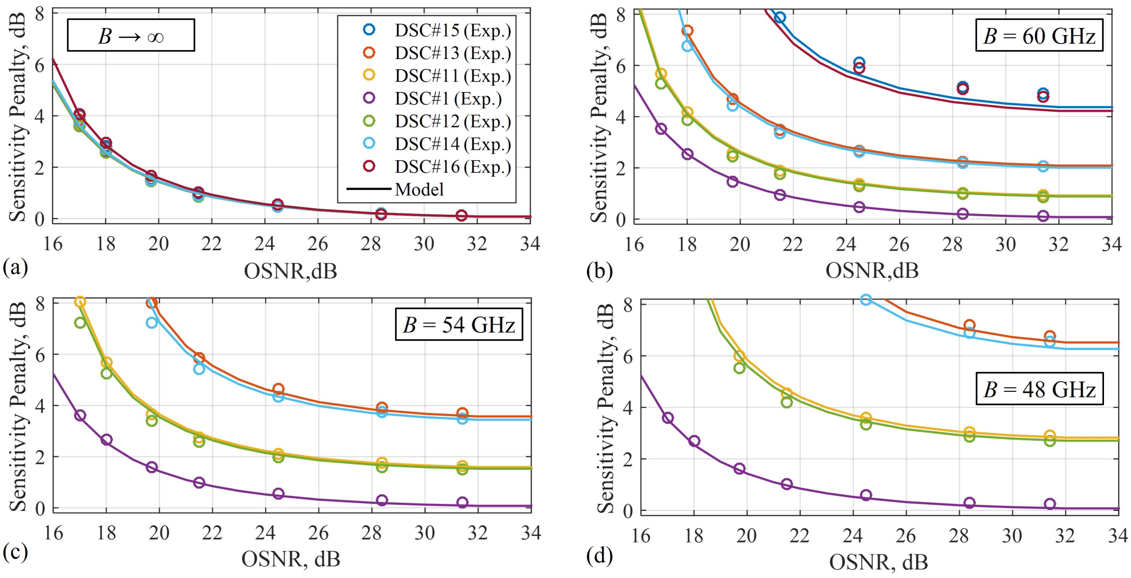

Fig. 2: (a) Experimental (in markers) versus analytical (in lines) sensitivity penalty as a function of OSNR (measured over a reference bandwidth equal to the DSC symbol rate) for representative subcarriers and setting different nominal filter B of (a) 5 THz, (b) 60 GHz, (c) 54 GHz, and (d) 48 GHz. Legend of (a) applies for (a)-(d).

5. Conclusions

We verified a model to predict the filtering impact on the performance of DSCM coherent systems, for a generic combination of ASE and TRX noises. We believe this model is useful in theoretical comparisons between single- and multi-carrier systems, thus allowing to improve the capabilities of physical-layer network planning tools.

Acknowledgments P. Torres-Ferrera, G. Parisi, C. Castro, R. Gaudino, G. Rizzelli and A. Napoli acknowledge support from the European Union's Horizon Europe research and innovation program, GA No. 101092766 (ALLEGRO).

References

1. G. Rizzelli *et al.*, "Experimental demonstration of in-field 400G coherent metro-access convergence," in *Optical Fiber Communications Conference and Exhibition (OFC)*, 2024, pp. 1–3.
2. I. Fernandez de Jauregui *et al.*, "An accurate model for system performance analysis of optical fibre networks with in-line filtering," in *European Conference on Optical Communication (ECOC)*, 2019, pp. 1–4.
3. G. Rizzelli *et al.*, "Filtering effects characterization in metro-access networks and future high-speed coherent optical communication schemes," *Journal of Lightwave Technology*, pp. 1–9, doi:10.1109/JLT.2024.3477552, 2024.
4. A. Ghazisaeidi *et al.*, "On the potential benefits of entropy-loading for digital multicarrier signals: Analytical assessment of quantization noise and bandwidth limitation impairments," in *OptoElectr. Comm. Conf. (OECC)*, 2022, pp. 1–4.
5. P. Torres-Ferrera *et al.*, "Analytical model for performance estimation of coherent digital subcarrier multiplexing systems affected by filtering, optical and electrical noise," in *Int. Conf. Transp. Opt. Netw. (ICTON)*, 2024, pp. 1–5.
6. T. Duthel *et al.*, "DSP design for coherent optical point-to-multipoint transmission," *Journal of Lightwave Technology*, vol. 42, no. 3, pp. 1109–1118, 2024.
7. L. Galdino *et al.*, "On the limits of digital back-propagation in the presence of transceiver noise," *Optics Express*, vol. 25, no. 4, pp. 4564–4578, 2017.
8. R. F. H. Fischer, *Linear Equalization*, ser. Precoding and Signal Shaping for Digital Transmission. Wiley, 2002.